Clinical assessment of retinal changes by spectral-domain OCT

Michele Iester[1], Sara Violanti[2], Luigi Borgia[2]

[1] Laboratorio Clinico Anatomo-funzionale per la Diagnosi e il Trattamento del Glaucoma e della Malattie Neurooftalmologiche, Clinica Oculistica, DiNOGMI, University of Genoa
[2] Is pre Oftalmica, Genoa - Italy

ABSTRACT

Purpose: To evaluate optical coherence tomography changes in patients with retinal thinning at the posterior pole.
Methods: In this cross-sectional and retrospective study, 648 files were reviewed, and 67 patients were selected. Optical coherence tomography images that showed an area with a retinal thickness reduction at the macular region by using the Asymmetry Analysis Map in Heidelberg Spectralis were selected. The presence of hemisphere asymmetry in the same eye and asymmetry between the paired eyes were calculated and used for the analysis. Retinal thickness was measured in 3 different retinal areas (squares): (1) the area (square) involved by the pathology (IA), (2) the specular area (square) in the opposite hemifield (SA), and (3) the corresponding IA in the contralateral eye (CIA) (area used to recruit the patients). Retinal layer morphology was analyzed observing the Spectralis screen.
Results: The thickness of the IA was 235.54 ± 39.95 µm (mean ± standard deviation), while it was 269.84 ± 36.16 µm and 293.81 ± 37.52 µm for SA and CIA, respectively.
Conclusions: Different retinal layers could be involved in reduction of the retinal thickness: a reduction of the inner layers was related to disease in which ciliary or retinal arterial vessel flow was involved, while a reduction of the outer retinal layer was related to pathologies related to choroidal flow diseases.

Keywords: Optic neuropathy, Retinal layer morphology, Retinal morphologic change, Vascular disease

Introduction

Patients with a decrease in retinal thickness can present several vision symptoms, such as blurred vision or change in contrast or color sensitivity. These symptoms can be found in several diseases related to disturbances of the cilioretinal and/or choroidal flow. These flow disturbances can also cause localized degenerative changes associated with thinning of the retina. Patients are often sent for an optical coherence tomography (OCT) scan to better understand the reason for visual change.

Imaging devices can assess the retinal structure and are able to give useful information. Spectral-domain OCT (SD-OCT) has the ability and the resolution to provide new information about retinal thickness and retinal layer morphology

that can aid diagnosis and management (1-5). Without these devices, it is not possible to establish which retinal layer is involved.

The aim of this study was to evaluate OCT changes in patients with retinal thinning at the posterior pole.

Patients and Methods

This retrospective, cross-sectional, observational study followed the principles of the Declaration of Helsinki. Institutional Review Board approval was not necessary because of its retrospective nature. Patients were imaged using the Heidelberg Spectralis HRA + OCT (Heidelberg Engineering, Heidelberg, Germany) in SD-OCT mode, using a scan field of 30 degrees horizontally and 15 degrees vertically and 19 to 25 OCT horizontal sections (one section at least every 240 µm). The Heidelberg Spectralis HRA and OCT (software version 1.6.1.0) can be used in any one of 6 imaging modes: SD-OCT, fluorescein angiography, indocyanine green angiography, autofluorescence, and red-free and infrared imaging. This article details use of the instrument in SD-OCT mode only. The Heidelberg Spectralis utilizes a broadband light source centered at 870 nm (i.e., no visible light "beacon") to simultaneously measure multiple wavelengths, a prerequisite of SD-OCT imaging. Simultaneous confocal scanning laser ophthalmoscopy is used to generate high-resolution
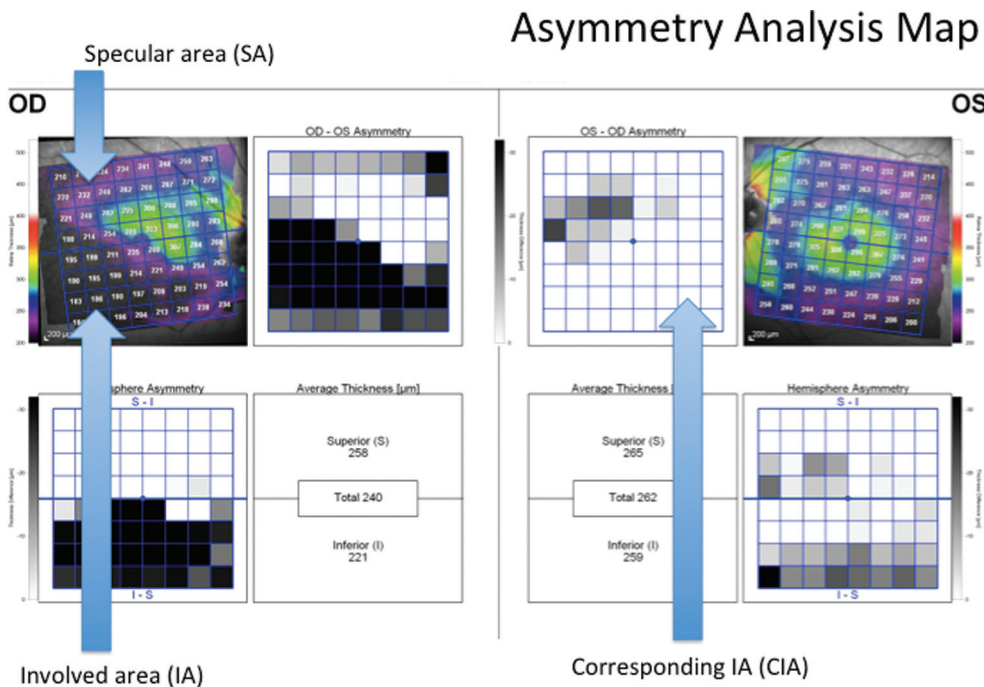
Fig. 1 - Printout of the Asymmetry Analysis Map: the user found the involved area and then the thinnest area was considered, together with the specular area and the corresponding area, as described in the text.

images of the retinal surface, thereby providing precise location information of each A-scan within a cross-sectional SD-OCT image. Spectral-domain OCT scanning generates 40,000 A-scans/s with an axial resolution of 3.5 μm/pixel digital (7 μm optical) and a transverse resolution of 14 μm (6). Alignment software continuously tracks any eye movement during image acquisition and then adjusts the position of the A-scan on the retinal surface to ensure accurate registration of cross-sectional OCT images. Using eye tracking and registration technology, multiple images are obtained from a precise location to then be averaged and filtered to remove random noise from the final image. The same eye tracking/registration technology is used to ensure that the instrument automatically rescans images that are influenced by blink artifacts. Similarly, follow-up images are derived from the same area of retina, thereby eliminating subjective placement of the scan by the operator.

Inclusion criteria

All the patients were referred for an OCT analysis, and only OCTs done from January 2011 to June 2012 were reviewed. The OCTs that showed an area with a retinal thickness reduction at the macular region by using the Asymmetry Analysis Map (AAM) in Heidelberg Spectralis were selected. In particular, when a retinal thickness difference was greater than 30 μm in an AAM square compared to the same located area of the paired eye, this difference was considered significant and the patient was recruited into the study. The presence of hemisphere asymmetry in the same eye and asymmetry between the paired eyes were calculated and used for the analysis. Retinal thickness was measured in 3 different retinal areas (squares): (1) the area (square) involved by the pathology (IA); (2) the specular

area (square) in the opposite hemifield (SA); and (3) the corresponding IA in the contralateral eye (CIA) (area used to recruit the patients) (Fig. 1).

Exclusion criteria

Patients with age-related macular degeneration, diabetic retinopathy, and/or vitreoretinal pathologies (i.e., macular hole and lamellar macular hole) were not included in the study, because these pathologies could create a significant retinal anatomical layer change. Patients with more than one ocular pathology (i.e., glaucoma and branch retinal artery occlusion [BRAO]) were not included in the study. Only one eye per patient was selected.

In this study, to find patients with retinal thinning by OCT, all OCT scans were reviewed, and only those with retinal thinning were selected. Then all the OCT scans were subjectively analyzed by 2 users just observing the Spectralis screen to distinguish which retinal layers were involved. The retinal thickness reduction was classified as internal when the ganglion cell complex (i.e., retinal nerve fiber, ganglion, inner plexiform, and nuclear layers) was involved, or external when the external layer (i.e., outer nuclear, outer plexiform, neuroepithelium, or pigment epithelium layers) was involved.

Statistical analysis

The data were analyzed by descriptive analysis and when the distribution of the data was normal, t test and Pearson r coefficient were used, while when the distribution of the data was non-normal, Mann-Whitney test and Spearman coefficient were used. Kruskal-Wallis test was used to compare the different subgroups. A p value <0.05 was considered significant.

Results

A total of 648 patient files were reviewed and 67 eyes of 67 patients were selected. Table I lists the details of the included patients. The thickness of the IA was 235.54 ± 39.95 µm (mean ± standard deviation), while it was 269.84 ± 36.16 µm and 293.81 ± 37.52 µm for SA and CIA, respectively (Tabs. II and III). A significant ($p<0.001$) difference was found between IA and both SA and CIA (Tab. II).

The retinal morphology was analyzed observing the OCT scans on the screen and 2 different subgroups of patients were found based on retinal involvement: a reduction of the inner layers or a reduction of the outer retinal layer. When eyes with a reduction of the inner layers were compared to those with a reduction of the outer retinal layer, no significant difference was found for IA and SA, except for CIA (Tab. IV). Then the diagnosis of each patient was considered and the group was divided into subgroups based on the diagnosis (Tab. III). No significant difference in retinal thickness was found among the diagnosis groups, but when the diagnosis was associated with retinal layer involvement, a significant difference was found among different pathologies. In particular, in all the optic neuropathy patients (primary open-angle glaucoma and anterior ischemic optic neuropathy) and

TABLE I - Descriptive analysis of the 6 subgroups

Disease	Age, y, mean (SD)	Number of eyes	Position (I vs E)
BRAO	72 (0.3)	2	I
rCSC	44.3 (6.9)	8	E
POAG	71 (12.1)	19	I
AION	71.7 (12.2)	15	I
Post PDT for CSC	73.3 (10)	3	E
CSE	64.3 (10.5)	20	E

AION = anterior ischemic optic neuropathy; BRAO = branch retinal artery occlusion; CSC = central serous chorioretinopathy; CSE = chronic serous epitheliopathy; E = external retinal layer involved; I = internal retinal layers involved; POAG = primary open angle glaucoma; PDT = photodynamic therapy; rCSC = resolved central serous chorioretinopathy.

TABLE II - Descriptive analysis of the entire cohort of patients

	Age	IA	SA	Difference (SA−IA)	CIA	Difference (CIA−IA)
Mean	66.29	235.54	269.84	34.47	293.81	58.00
SD	13.42	39.95	36.16	29.69	37.52	25.83
p Value				IA vs SA <0.001		CIA vs IA <0.001

CIA = the corresponding area involved by the pathology in the contralateral eye; IA = the area involved by the pathology; SA = the specular area in the opposite hemifield.

TABLE III - Comparison among the different diagnosis subgroups

Disease	IA	SA	Difference (SA−IA)	CIA	Difference (CIA−IA)
rCSC	243.13 (39.68)	247.38 (36.02)	31.25 (24.78)	307 (47.02)	63.88 (27.67)
POAG	235.37 (26.50)	267.74 (25.07)	32.32 (20.67)	281.89 (31.44)	48.28 (17.32)
AION	246.93 (29.87)	275.33 (34.78)	28.6 (29.89)	292.4 (29.17)	45.47 (22.15)
CSE	232.3 (48.09)	269.05 (40.96)	36.75 (34.78)	306.65 (38.96)	71.85 (28.88)
Post PDT	264.7 (54.24)	309 (32.19)	44.33 (29.02)	312.3 (47.12)	47.67 (8.74)
BRAO	210.5 (34.65)	259 (36.77)	53.5 (9.19)	261.5 (50.2)	51 (15.56)

AION = anterior ischemic optic neuropathy; BRAO = branch retinal artery occlusion; CIA = the corresponding area involved by the pathology in the contralateral eye; CSE = central serous epitheliopathy; IA = the area involved by the pathology; PDT = photodynamic therapy; POAG = primary open-angle glaucoma; rCSC = resolved central serous chorioretinopathy; SA = the specular area in the opposite hemifield.

TABLE IV - Comparison between patients with internal retinal layers involved and those with external retinal layer involved

	IA	SA	Difference (SA−IA)	CIA	Difference (CIA−IA)
External layer					
Mean	238.23	274.29	36.06	307.29	67.45
SD	46.13	39.66	33.43	40.36	27.71
p Value	0.475	0.324	0.282	0.008	<0.001
Internal layer					
Mean	238.81	270.42	31.94	285.23	47.23
SD	28.86	29.45	24.72	31.31	19.03

CIA = the corresponding area involved by the pathology in the contralateral eye; IA = the area involved by the pathology; SA = the specular area in the opposite hemifield.

in those with BRAO, a reduction of the ganglion cell complex was observed (Figs 2-4) while in patients with resolved central serous chorioretinopathy, post photodynamic therapy, and chronic serous epitheliopathy, a reduction of the outer retinal layer was observed (Figs. 5-7).
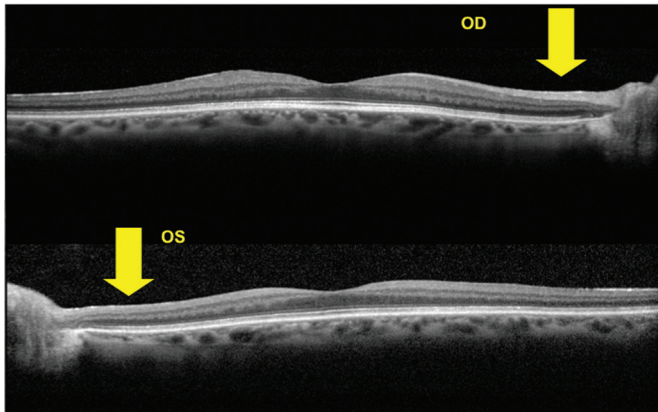
Discussion

Optical coherence tomography in clinical practice has improved the imaging of the retina with better morphologic and morphometric information. Previous studies have shown that SD-OCT reveals retinal pathology that was not visible using
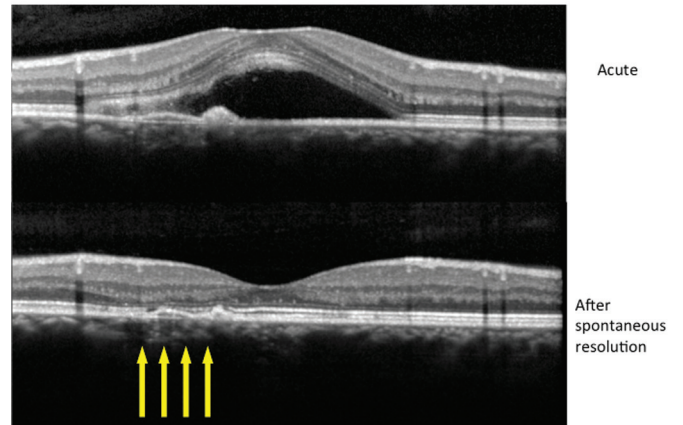
Left - Anterior Ischemic Optic Neuropathy

Reduction of ganglion cell complex (RNFL and ganglion cell layer)

Fig. 2 - Patient with left anterior ischemic optic neuropathy: reduction of ganglion cell complex (retinal nerve fiber layer and ganglion cell layer).
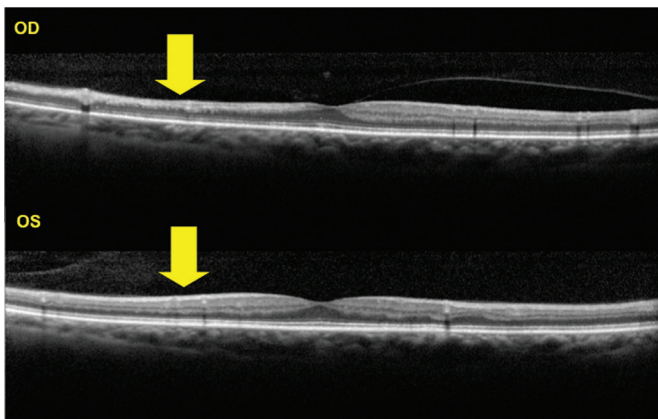
Right – Branch Retinal Artery Occlusion

Reduction of inner retinal layers up to the outer plexiform layer

Fig. 3 - Patient with right branch retinal artery occlusion: reduction of inner retinal layers up to the outer plexiform layer.

Right – Primary Open Angle Glaucoma

Reduction of ganglion cell complex

Fig. 4 - Patient with right primary open-angle glaucoma: reduction of ganglion cell complex.

Right - Central Serous Corioretinopathy

Reduction of outer nuclear layer and neuroepithelium/RPE dystrophy

Fig. 5 - Patient with right central serous chorioretinopathy: reduction of outer nuclear layer and neuroepithelium/retinal pigment epithelium dystrophy.
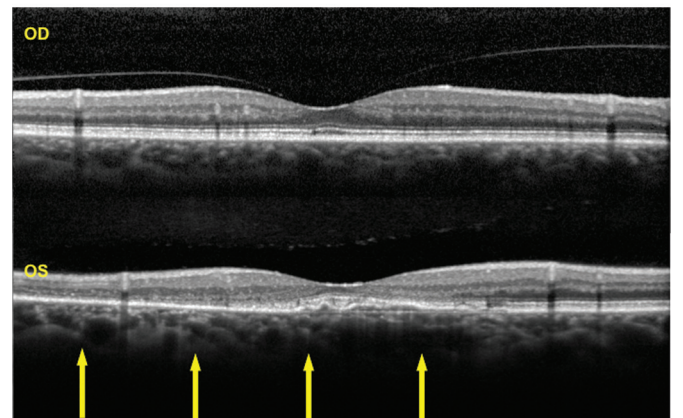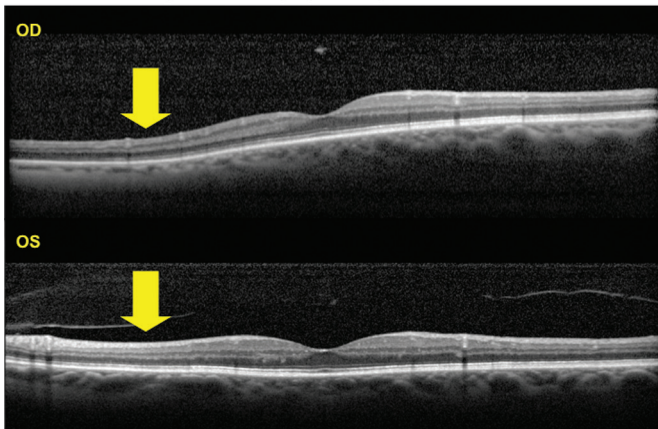
Left - Chronic Serous Epitheliopathy

Reduction of neuroepithelium, outer nuclear and plexiform layers

Fig. 6 - Patient with left chronic serous epitheliopathy: reduction of neuroepithelium and outer nuclear and plexiform layers.
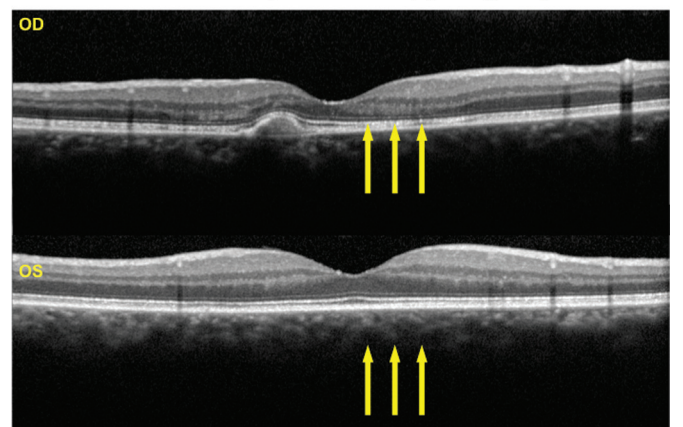
After Photo Dynamic Therapy in right eye

Reduction of outer nuclear layer

Fig. 7 - Patient after photodynamic therapy in right eye: reduction of outer nuclear layer.

time-domain OCT, such as intraretinal cysts and subretinal fluid (7). Spectral-domain OCT also adds information to complete the clinical picture, providing more detailed resolution of retinal changes, such as full-thickness folds of the retinal pigment epithelium (RPE) and intraretinal edema in case of RPE detachment, branch retinal vein occlusion, toxoplasma chorioretinitis, and polypoidal choroidal vasculopathy (8).

In this study, high OCT resolution was used to better understand retinal layers involvement in different diseases (3, 5). From morphologic observation of the scans, a thinning of the ganglion cell complex layers and the inner plexiform layer was found in patients with ganglion cell complex diseases such as ONH diseases as well as in patients with retinal artery disease. On the other hand, in patients with retinal pathologies in which the choroidal flow was involved, an outer nuclear layer, outer plexiform layer, and/or neuroepithelium thinning was observed. Ghazi et al (9) found that a loss of the inner retinal layer could differentiate postacute retinal artery occlusion from nonacute optic neuropathy, confirming part of our results.

The ability of SD-OCT to clearly and objectively elucidate subtle morphologic changes within the retinal layers provides information that could be useful to better explain patients' symptoms. The ability to evaluate each retinal layer permits better assessment of the retinal reduction and understanding of the location of the damage in the vision pathway. However, in this study, no difference in retinal thickness was found among patients with different diseases; we could not perform an automatic segmentation analysis, and we assessed the retinal layers all together.

A significant difference was found between the area with the disease (IA) and the specular area across the hemi-meridian (SA) and the corresponding area in the other eye (CIA), suggesting that all these patients had retinal thinning due to their diseases.

When the subgroup with inner retinal thinning was compared to that with outer retinal thinning, no difference was found for IA and SA, but for CIA a significant difference was found between the 2 subgroups. These data could be explained because ONH disease and artery disease are mainly systemic diseases and both eyes could be involved in different ways. Indeed, the retinal thickness was thinner in the subgroup with inner thinning. Furthermore, in the post photodynamic therapy subgroup, all patients had a retinal thinning of the outer layers, where the treatment was focused.

A possible bias of this study could be that in healthy subjects the retinal thickness is similar in the IA, SA, and CA; however, we selected areas, and not points, that had a retinal reduction in the AAM. The utility of the areas could guarantee a good clinical judgment even if the measurement was less accurate for the noise in the measurement. Other possible biases could be the design of the study (cross-sectional), the selection of patients (inclusion and exclusion criteria), and the number of included patients, but we tried to avoid any clinical noise among the selected patients by using strict inclusion/exclusion criteria.

We selected patients on the basis of the retinal thinning and not the disease, because from the clinical point of view, patients are sent for an OCT scan without any diagnosis. This could be a bias for the study because the sample selected could be too heterogeneous, but on the other hand, these data could help the OCT user to read the scan and make the diagnosis. Besides the ability of SD-OCT to elucidate clearly and objectively subtle morphologic changes within the retinal layers, it provides information that could be used to confirm diagnoses with greater confidence. Because this imaging technology offers a previously unattainable resolution of retinal morphology, a more accurate intraretinal diagnosis could be done in the future.

In conclusion, we showed that if there is retinal thinning by OCT, it is important to evaluate which retinal layer is involved: a reduction of the inner layers was related to disease in which ciliary or retinal arterial vessel flow was involved, while a reduction of the outer retinal layer was related to pathologies related to choroidal flow diseases. The possibility to use a retinal segmentation program to assess objectively morphologic changes within the retinal layers that are not visible using conventional clinical techniques could be useful in clinical practice. (Figs. 4-7).

Disclosures

References

1. Hassenstein A, Meyer CH. Clinical use and research applications of Heidelberg retinal angiography and spectral-domain optical coherence tomography: a review. Clin Experiment Ophthalmol. 2009;37:130-43.
2. Helb HM, Charbel Issa P, Fleckenstein M, et al. Clinical evaluation of simultaneous confocal scanning laser ophthalmoscopy imaging combined with high-resolution, spectral-domain optical coherence tomography. Acta Ophthalmol. 2010;88:842-9.
3. Drexler W. Cellular and functional optical coherence tomography of the human retina: the Cogan lecture. Invest Ophthalmol Vis Sci. 2007;48:5339-51.
4. Drexler W, Fujimoto JG. State-of-the-art retinal optical coherence tomography. Prog Retin Eye Res. 2008;27:45-88.
5. de Boer JF, Cense B, Park BH, Pierce MC, Tearney GJ, Bouma BE. Improved signal-to-noise ratio in spectral-domain compared with time-domain optical coherence tomography. Opt Lett. 2003;28:2067-9.
6. Heidelberg Engineering. Spectralis Hardware Operating Instructions: Technical Specifications. Heidelberg: Heidelberg Engineering; 2007: 22-5.
7. Luviano DM, Benz MS, Kim RY, et al. Selected clinical comparisons of spectral domain and time domain optical coherence tomography. Ophthalmic Surg Lasers Imaging. 2009;40:325-8.
8. Singh M, Chee CKL. Spectral domain optical coherence tomography imaging of retinal diseases in Singapore. Ophthalmic Surg Lasers Imaging. 2009;40:336-41.
9. Ghazi NG, Tilton EP, Patel B, Knape RM, Newman SA. Comparison of macular optical coherence tomography findings between postacute retinal artery occlusion and nonacute optic neuropathy. Retina. 2010;30:578-85.